

On the Probability of False Alarm of the Power Spectral Density Split Cancellation Method

Roberto C. D. V. Bomfim, Dayan A. Guimarães, *Member, IEEE*, and Rausley A. A. de Souza, *Member, IEEE*

Abstract—The cooperative power spectral density split cancellation (CPSC) method was recently proposed for cooperative spectrum sensing, with the novelties of being robust against noise uncertainty and having low computational complexity. The probability of false alarm has been derived in the related paper, but under assumptions that make it inaccurate. In this letter we derive the correct cumulative distribution functions of the main random variables that form the decision statistic of the CPSC model. We also derive the correlation coefficient between sub-band decisions, a necessary information that was neglected in the reference paper, leading to an expression for the final probability of false alarm that is more accurate than the original one. Our theoretical results are validated with simulations.

Index Terms—Cognitive radio, cooperative power spectral density split cancellation, spectrum sensing.

I. INTRODUCTION

THE cognitive radio (CR) concept has emerged as a potential solution for the scarcity and idleness of the electromagnetic spectrum in wireless communication systems [1]. Among a myriad of cognitive tasks, the spectrum sensing is the one that enables the opportunistic access of the CRs of a secondary network to the vacant bands of a primary network. Cooperative spectrum sensing (CSS) techniques have been developed to reduce the complexity of the CR and to mitigate channel impairments in order to improve performance, taking advantage of spatial diversity [2]. In centralized CSS schemes, the sensor information from the CRs are combined at the fusion center (FC) of the CR network, where the final decision upon the occupation of the sensed band is made. The information that the CRs send to the FC can be either individual CR decisions or some soft information derived from samples of the signals received by the CRs. The former is known as decision fusion and the latter is usually referred to as data fusion.

The present paper considers the cooperative power spectral density split cancellation (CPSC) method proposed in [3], which can be cast as a data fusion scheme. The most important characteristics of this method are the low computational complexity and the robustness against dynamical noise, or noise uncertainty. In [3], the authors present the CPSC algorithm, give the stochastic properties of the power spectral density (PSD) of the received signal, derive the expressions for the probability of false alarm (PFA) and the decision threshold,

and show simulation results in terms of the receiver operating characteristic (ROC) curves, attesting the robustness of the method under dynamical noise.

Here we derive the cumulative density functions (CDFs) of the random variables that form the decision statistic of the CPSC model, showing that the corresponding ones as given in [3] are not correct. Specifically, we consider the influence of the correlation coefficient between these random variables. We also derive the correlation coefficient between the random variables that are associated to the CR decisions in the sub-band level. These correlations were not taken into account in [3], but we point out that they are intrinsic to the CPSC method. By neglecting them, inaccurate PFA results are produced. An approximate, yet more accurate expression for the PFA is also derived here, and verified against simulation results. Additionally, the CPSC method is generalized in this letter by considering both symmetric and non symmetric PSDs; originally, only symmetric PSDs were assumed.

The remaining of the paper is organized as follows: Section II briefly describes the CPSC method and give the main definitions from [3] that allow for the readability of the rest of the manuscript. The new CDFs related to the PFA and the new expression for the PFA are derived in Section III. In Section IV our theoretical results are contrasted with simulations and with those obtained from the expressions in [3]. Section V concludes the paper. For the sake of consistence, the same notation of [3] is adopted here.

II. THE ORIGINAL CPSC METHOD

Consider that the received signal $x_u(t)$ [3, eq. (1)] at the u -th CR, $u = 1, 2, \dots, U$ is sampled, producing a discrete-time signal $x_u(n)$, $n = 0, 1, \dots, M - 1$, being M the number of samples collected by each CR. Briefly, the CPSC method follows the steps: 1) Estimate the PSD of $x_u(n)$ as $F_u(k)$, $k = 0, 1, \dots, M - 1$ [3, eq. (3)]; 2) Divide $F_u(k)$ into L sub-bands with V elements in each, so $V = M/L$, such that M and V are even. For each CR, the power in the total (full) band and in the l -th sub-band, $l = 1, 2, \dots, L$, are respectively computed from $F_{full,u} = \sum_{k=1}^{M/2} F_u(k)$ and $F_{l,u} = \sum_{k=1}^{V/2} F_u[(l-1)V + k]$; 3) To cancel the noise effect, compute $r_u(l) = F_{l,u}/F_{full,u}$ for each sub-band and each CR; 4) Average $r_u(l)$ over all CRs to obtain the decision variable (or test statistic) for each sub-band, $r_{avg}(l)$ [3, eq. (7)]; 5) Compare $r_{avg}(l)$ to the decision threshold γ in order to decide upon each sub-band occupation, according to [3, eq. (8)]; and finally 6) Make the final decision according to the rule in [3, eq. (9)].

Writing $Z = r_u(l)$ for notational simplicity, the conditional CDF of Z under the null hypothesis, $P[Z < z | \mathcal{H}_0] =$

Roberto C. D. V. Bomfim, Dayan A. Guimarães, and Rausley A. A. de Souza are with the National Institute of Telecommunications (Inatel), PO Box 05, 37540-000 Santa Rita do Sapucaí - MG - Brazil (Tel:+55 (35) 3471 9227, Fax:+55 (35) 3471 9314, e-mail: roberto@gee.inatel.br, dayan@inatel.br, rausley@inatel.br)

$C_u(z|\mathcal{H}_0)$, is given in [3, eq. (28)], and the PFA, $P_{f,i}(\gamma)$, for each sub-band is given by [3, eq. (30)]. The global PFA, $P_f(\gamma)$, is then computed from [3, eq. (31)].

III. NEW EXPRESSIONS IN THE CPSC METHOD

In this section, new expressions for the CDFs of $r_u(l)$ and $r_{avg}(l)$ are derived. A new expression for the global PFA is derived as well. From these expressions and from the results presented later on in this paper one can infer on the inaccuracies of [3, eqs. (28), (30), (31) and (32)].

A. Cumulative distribution functions

The thermal noise term in the model proposed in [3] is a circular symmetric complex Gaussian (CSCG), independent and identically distributed (i.i.d.) random process with variance σ_u^2 , not necessarily identical for different CRs. The n -th sample of the noise waveform at the u -th CR is $w_u(n) = w_u^r(n) + jw_u^i(n)$, where the superscripts denote the real (r) and the imaginary (i) part of the noise, which are both zero mean Gaussian random variables with variance $\sigma_u^2/2$, and independent from each other.

The first point to consider is that the summations that form $F_{full,u}$ and $F_{l,u}$ consider $M/2$ and $V/2$ terms respectively, under the assumption that the PSD $F_u(k)$ is symmetric. However, in order to make the CPSC method more general, it is considered here the summations of $S \times M$ and $S \times V$ terms, respectively, with $S = 0.5$ in the case of a symmetric $F_u(k)$, and $S = 1$ otherwise. So, $F_{full,u}$ and $F_{l,u}$ become respectively $F_{full,u} = \sum_{k=1}^{M \times S} F_u(k)$ and $F_{l,u} = \sum_{k=1}^{V \times S} F_u[(l-1)V + k]$. Denoting the expectation and variance operators respectively by $\mathbb{E}(\cdot)$ and $\mathbb{V}(\cdot)$, from [3] we have $\mathbb{E}[F_u(k)|\mathcal{H}_0] = \sigma_u^2$ and $\mathbb{V}[F_u(k)|\mathcal{H}_0] = \sigma_u^4$. Then, it is easy to see that $\mathbb{E}[F_{full,u}|\mathcal{H}_0] = S \times M\sigma_u^2$, $\mathbb{V}[F_{full,u}|\mathcal{H}_0] = S \times M\sigma_u^4$, $\mathbb{E}[F_{l,u}|\mathcal{H}_0] = S \times V\sigma_u^2$ and $\mathbb{V}[F_{l,u}|\mathcal{H}_0] = S \times V\sigma_u^4$. Once again, in the case of $S = 0.5$ these last four values specialize to those reported in [3].

For large values of M and V , $F_{full,u}$ and $F_{l,u}$ will tend to be Gaussian random variables according to the central limit theorem (CLT), an assumption also adopted in [3]. Then, $r_u(l)$ will be the ratio of two Gaussian random variables. The CDF of this ratio, as given in [4, eq. (4)], is

$$P[Z < z|\mathcal{H}_0] = 1 - Q\left(\frac{\mu_2 z - \mu_1}{\sigma_1 \sigma_2 a(z)}\right), \quad (1)$$

where $Q(x) = \int_x^\infty \frac{1}{\sqrt{2\pi}} \exp(-\frac{1}{2}t^2) dt$, μ_1 and μ_2 are respectively the mean of the variables $F_{l,u}$ and $F_{full,u}$, and σ_1 and σ_2 are the corresponding standard deviations, with

$$a(z) = \sqrt{\frac{z^2}{\sigma_1^2} - \frac{2\rho z}{\sigma_1 \sigma_2} + \frac{1}{\sigma_2^2}}, \quad (2)$$

where ρ is the correlation coefficient between $F_{l,u}$ and $F_{full,u}$. This correlation coefficient has been neglected in [3], and we have found it to be (see Appendix A)

$$\rho = 1/\sqrt{L}. \quad (3)$$

It is worth mentioning that equation (1) is a simplification which assumes that $\sigma_2 \ll \mu_2$. In the present derivation, it

corresponds to assuming that $\sqrt{SM\sigma_u^4} \ll SM\sigma_u^2$, which is a reasonable assumption, specially as M gets larger (recall that a large M has already been an assumption here and in [3] so that the CLT applies to the distribution of $F_{l,u}$ and $F_{full,u}$).

By substituting the mean and the standard deviation of $F_{l,u}$ and $F_{full,u}$ in (1), the correct CDF of $r_u(l)$, that is $P[Z < z|\mathcal{H}_0]$, is given by

$$C_u(z|\mathcal{H}_0) = Q\left(\sqrt{S} \frac{V - Mz}{\sqrt{Mz^2 - 2Vz + V}}\right). \quad (4)$$

One can see that (4) does not become equal to [3, eq. (28)] by setting $S = 0.5$. To arrive at the CDF of $r_{avg}(l)$, and consequently $P_{f,i}(\gamma)$, as in [3] we have used the fact that this CDF obeys the same distribution of $\sum_{u=1}^U F_{l,u} / \sum_{u=1}^U F_{full,u}$. Under the same reasoning adopted to derive (4), the correct PFA in each sub-band is given by

$$P_{f,i}(\gamma) = 1 - Q\left(\sqrt{SU} \frac{V - M\gamma}{\sqrt{M\gamma^2 - 2V\gamma + V}}\right), \quad (5)$$

where the second term in the right-hand part is the CDF of $r_{avg}(l)$. In this case it is also clear that setting $S = 0.5$ does not make (5) equal to [3, eq. (30)].

Therefore, equations (4) and (5) unveil that the results given in [3, eq. (28) and (30)], respectively, do not correspond to the random variables to which they are related.

B. Final probability of false alarm

The correlation between $F_{l,u}$ and $F_{full,u}$ derived in the Appendix A also influences the global PFA through the way that the associated CDFs are operated in the final expression for the PFA. Specifically in the case of the expression [3, eq. (31)], we have also found that it is not taking into consideration this correlation. This can be concluded by noticing firstly that this expression results as the probability of at least 1 success in L *uncorrelated* binary (Bernoulli) trials. The successes correspond to false alarm events at the sub-band level, i.e. deciding in favor of \mathcal{H}_1 given \mathcal{H}_0 for each sub-band; see [3, eq. (8)]. However, these events are *correlated*, since $r_{avg}(l)$ and $r_{avg}(i)$ are correlated for $l \neq i$. This is immediate from the definition of $r_{avg}(l)$ in [3, eq. (7)], and from the nonzero correlation coefficient between $F_{l,u}$ and $F_{full,u}$, i.e. $\rho = 1/\sqrt{L}$. One must recall that, even if [3, eq. (31)] were originally written to consider that the implicit Bernoulli trials were correlated, the use of the inaccurate CDFs [3, eqs. (28) and (30)] would still produce inaccurate results. In what follows we give a correct, yet approximated derivation of the global PFA from the joint cumulative distribution function (JCDF) of the decision variables at the sub-band level, which completely takes into account the level of correlation between $r_{avg}(l)$ and $r_{avg}(i)$.

Consider the random vector $\mathbf{R} = [R_1, R_2, \dots, R_L]^T$, where $[\cdot]^T$ means transpose, and where the elements are $R_l = r_{avg}(l)$, $l = 1, 2, \dots, L$, for the sake of notational simplification. The JCDF of \mathbf{R} is defined as $F_{\mathbf{R}}(\mathbf{r}) \triangleq F_{R_1, R_2, \dots, R_L}(r_1, r_2, \dots, r_L)$, with r_1, r_2, \dots, r_L corresponding to the decision threshold γ . From the final decision rule [3, eq. (9)], one can see that $F_{\mathbf{R}}(\mathbf{r})$ corresponds to the probability

that the final decision is in favor of \mathcal{H}_0 and, therefore, the global PFA can be written as

$$P_f(\gamma) = 1 - F_{R_1, R_2, \dots, R_L}(\gamma, \gamma, \dots, \gamma | \mathcal{H}_0). \quad (6)$$

If it is considered that the decisions at the sub-band level are independent of each other, which means independence among the elements of \mathbf{R} , equation (6) is simplified to [3, eq. (31)]. However, it was found that any two elements R_l and R_i of \mathbf{R} , for $l \neq i$, exhibit a correlation coefficient of (see Appendix B)

$$\rho_{R_l R_i} = -1/(L - 1), \quad (7)$$

from where one can see that $\rho_{R_l R_i}$ approaches zero as the number of sub-bands L increases, as expected. For small values of L , [3, eq. (31)] becomes not valid because $F_{R_1, R_2, \dots, R_L}(\gamma, \gamma, \dots, \gamma | \mathcal{H}_0)$ can not be written as the CDF of R_l raised to the L -th power.

The probability density function (PDF) of R_l , denoted by $f_R(\gamma)$, can also be derived considering the simplified PDF of the ratio of two Gaussian random variables as given in [4, eq. (9)], in which we have replaced the mean and the standard deviation of $\sum_{u=1}^U F_{l,u}$ and $\sum_{u=1}^U F_{full,u}$, and the correlation between them, $\rho = 1/\sqrt{L}$. The result PDF turned out to be

$$f_R(\gamma) = \frac{ab\sqrt{2}\exp[a/(\gamma^2 - 2\gamma/L + 1/L)]}{\sqrt{USM\pi}(\gamma^2 - 2\gamma/L + 1/L)^{3/2}}, \quad (8)$$

where $a = SUV(1 - 1/L)/2$ and $b = \exp[-2SU(M - V)/(4(1 - 1/L))]$.

Although $f_R(\gamma)$ is not Gaussian, we have generated and analyzed 100000 samples of R_l under several system parameters and observed that it fits a Gaussian random variable with a p -value of 0.48 or higher under the Kolmogorov-Smirnov goodness-of-fit test. In this case its variance can be computed as $\sigma_{R_l}^2 = \mathbb{E}[R_l^2] - \mathbb{E}^2[R_l]$, in which $\mathbb{E}^2[R_l] = 1/L^2$ and $\mathbb{E}[R_l^2]$ is calculated numerically as $\mathbb{E}[R_l^2] = \int_{-\infty}^{\infty} \gamma^2 f_R(\gamma) d\gamma$.

Then, it is possible to arrive at an approximate expression for the joint PDF (JPDF) of \mathbf{R} , as given by the Gaussian JPDF

$$f_{\mathbf{R}}(r_1, r_2, \dots, r_L | \mathcal{H}_0) = \frac{1}{\sqrt{(2\pi)^L |\boldsymbol{\Sigma}|}} \exp\left(-\frac{1}{2} (\mathbf{r} - 1/L)^T \boldsymbol{\Sigma}^{-1} (\mathbf{r} - 1/L)\right), \quad (9)$$

where $\mathbf{r} = [r_1, r_2, \dots, r_L]^T$, with elements r_1, r_2, \dots, r_L corresponding to the decision threshold γ in [3, eq. (8)]. $|\boldsymbol{\Sigma}|$ is the determinant of the covariance matrix $\boldsymbol{\Sigma}$, whose diagonal elements are $\sigma_{r_{avg}}^2$ and the off-diagonal elements are $\rho_{R_l R_i} \sigma_{r_{avg}}^2$, with $\rho_{R_l R_i}$ obtained from (7). The JCDF of \mathbf{R} is then given by

$$F_{\mathbf{R}}(r_1, r_2, \dots, r_L | \mathcal{H}_0) = \int_{-\infty}^{r_1} \dots \int_{-\infty}^{r_L} f_{\mathbf{R}}(r'_1, r'_2, \dots, r'_L | \mathcal{H}_0) dr'_1 dr'_2 \dots dr'_L, \quad (10)$$

which can be solved numerically. Finally, the approximate global PFA can be found by operating equation (9) in (10), and then operating the result in (6).

Obviously, since the expression [3, eq. (31)] is not correct, the expression for the decision threshold γ given in [3, eq. (32)] is also inexact.

IV. NUMERICAL RESULTS

This section aims at validating the expressions derived in this paper, which are the CDFs of $r_u(l)$ and $r_{avg}(l)$, and the approximate expression for the PFA, also comparing results obtained from these expressions and those obtained from the original expressions in [3]. To do so, the CPSC method was simulated under the \mathcal{H}_0 hypothesis via 20000 Monte Carlo events. We have set $M = 1000$, $L = 5$ and $U = 5$. Considering that the noise signal is complex, its PSD is non-symmetric, therefore we have set $S = 1$; the same conclusions drawn from this case also apply when $S = 0.5$. Notice that to use $S = 0.5$, the received signal at the CRs must be real.

Fig. 1 shows the CDFs of $r_u(l)$ and $r_{avg}(l)$ as given respectively by [3, eq. (28)] and the second term in the right-hand side of [3, eq. (30)], along with the corresponding CDFs derived in this paper, that is, (4) and the second term in the right-hand side of (5). The associated empirical CDFs from simulations are also shown, considering $l = 1$ without loss of generality. We point out that to plot the theoretical results from [3], we have set $M = 2000$ because the original expressions consider $S = 0.5$ (refer to Subsection III-A). From Fig. 1 it is clear the adherence between the simulation results and those obtained from the CDFs derived in this paper. It is also evident the large discrepancy between the CDF of $r_u(l)$ derived [3] and the corresponding CDF derived in this paper. Regarding the CDF of $r_{avg}(l)$, the discrepancy is less pronounced, though it can be seen by magnifying the curves.

In terms of performance, Fig. 2 presents ROC curves in which the probability of detection P_d was computed from the empirical CDF of the test statistic [3, eq. (7)] under the hypothesis \mathcal{H}_1 , and the probability of false alarm P_f was computed using the associated expressions from [3] and those derived here. Monte Carlo simulation results are also shown. The signal-to-noise (SNR) ratio at the CRs was set to -10 dB in the case of $M = 1000$ and $L = 5$, and it was set to -25 dB in the case of $M = 50000$ and $L = 25$. To plot the corresponding theoretical results from [3], we have respectively set $M = 2000$ and $M = 100000$. For $M = 1000$ and $L = 5$, it is clear from this figure that our result is in agreement with the simulation, whereas the result obtained from the expressions in [3] is considerably inaccurate and overestimates the spectrum sensing performance.

If M is large and L is further increased, with $V = M/L$ large, then ρ and $\rho_{R_l R_i}$ will tend to zero. In this case, the expressions derived in [3] become valid, and the theoretical results obtained from [3] tend to merge with ours and with the simulations, as shown in Fig. 2 when $M = 50000$ and $L = 25$, mainly at low values of PFA.

For small L , as M is decreased our results and those from [3] are still different from one another, but they tend to depart from the simulations because the CLT becomes not applicable, since the sub-band decision variable will tend to exhibit a less Gaussian behavior. In this case, however, our results stay closer to the simulations than those from [3]. This can be verified in Fig. 3, in the group of ROC curves associated to $L = 5$. For this figure $M = 100$ and the remaining parameters are identical to those adopted in the case of Fig. 2. Again, the

result obtained from the expressions in [3] overestimates the spectrum sensing performance.

Now, if L is increased and the remaining parameters are kept as in the previous paragraph, our results and the ones from [3] merge, but they depart from the simulations, again due to the noncompliance with the CLT. This situation can be seen in Fig. 3, in the group of ROC curves associated to $L = 25$.

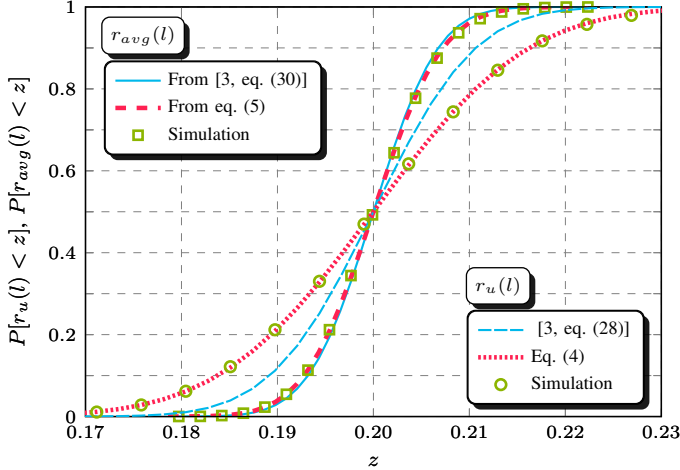


Fig. 1. CDFs of $r_u(l)$ and $r_{avg}(l)$ for $M = 1000$, $L = 5$ and $U = 5$.

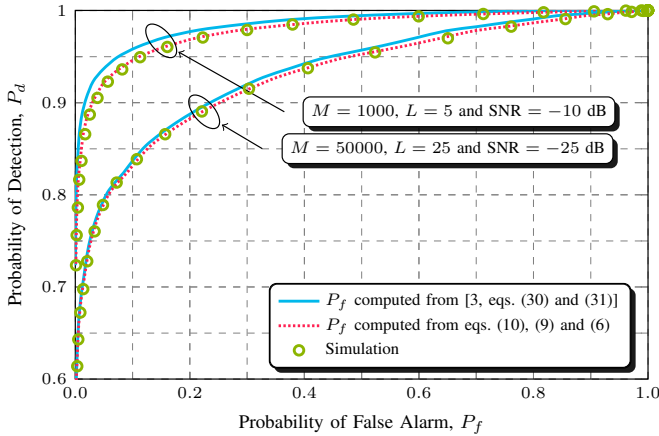


Fig. 2. ROC curves for different values of SNR, M and L with $U = 5$.

V. CONCLUSIONS

The intrinsic correlations associated with the random variables that form the test statistic of the CPSC method were not taken into account in [3], resulting in inaccurate expressions. By taking into account these correlations, in this letter we derived more accurate expressions and validated them against simulation results. Given the robustness against noise uncertainty and the low computational complexity of the CPSC method, new deployments of it are to come and will benefit from the expressions derived here.

ACKNOWLEDGMENT

This work partially supported by Finep (with Funtel resources), Grant 01.14.0231.00, under the Radiocommunications Reference Center (*Centro de Referência em*

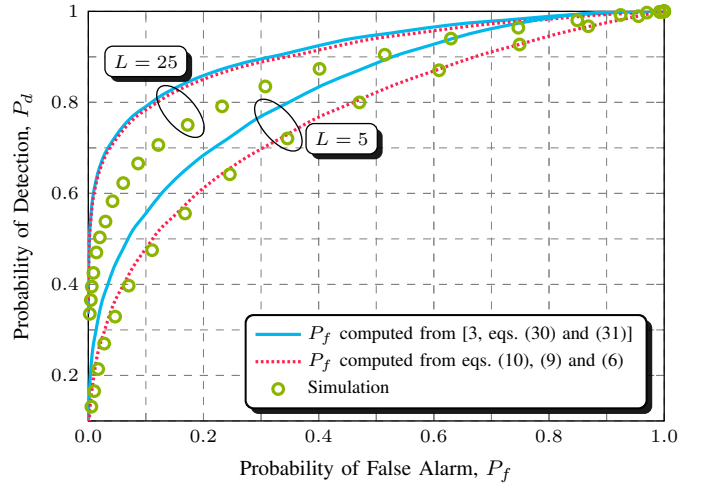


Fig. 3. ROC curves for SNR = -10 dB, $M = 100$, $L = 5$ and 25 , and $U = 5$.

Radiocomunicações, CRR) project of the National Institute of Telecommunications (*Instituto Nacional de Telecomunicações*, Inatel), Brazil.

APPENDIX A

CORRELATION COEFFICIENT BETWEEN $F_{l,u}$ AND $F_{full,u}$

For notational simplicity, let us define the random variables $X = F_{l,u}$, $Y = F_{full,u}$ and $W = Y - X$. If $\mathbb{V}[X] = \sigma_x^2$, then $\mathbb{V}[Y] = L \times \sigma_x^2$, since there are L sub-bands and $F_{l,u}$ is independent of $F_{i,u}$ for $l \neq i$. The correlation coefficient between X and Y is then $\rho = (\mathbb{E}[XY] - \mathbb{E}[X]\mathbb{E}[Y]) / \sqrt{\mathbb{V}[X]\mathbb{V}[Y]}$, which can be rewritten as

$$\rho = (\mathbb{E}[X^2] + \mathbb{E}[XW] - \mathbb{E}^2[X] - \mathbb{E}[X]\mathbb{E}[W]) / (\sigma_x^2 \sqrt{L}). \quad (11)$$

Using the fact that $\mathbb{E}[XW] = \mathbb{E}[X]\mathbb{E}[W]$ from the independence between $F_{l,u}$ and $F_{i,u}$ for $l \neq i$, and the identity $\mathbb{E}[X^2] - \mathbb{E}^2[X] = \sigma_x^2$, then (11) simplifies to (3).

APPENDIX B

CORRELATION COEFFICIENT BETWEEN R_l AND R_i

The correlation coefficient between R_l and R_i is

$$\rho_{R_l R_i} = (\mathbb{E}[R_l R_i] - \mathbb{E}^2[R_l]) / (\mathbb{E}[R_l^2] - \mathbb{E}^2[R_l]). \quad (12)$$

From [3, eqs. (6) and (7)] one can realize that $\sum_{l=1}^L R_l = \sum_{l=1}^L r_{avg}(l) = 1$. Then $R_i = 1 - \sum_{l=1, l \neq i}^L R_l$, from where, under the reasonable assumption that $\mathbb{E}[R_1] = \mathbb{E}[R_2] \dots = \mathbb{E}[R_L]$, one obtains $\mathbb{E}[R_i] = 1/L$ and $\mathbb{E}[R_l R_i] = (\mathbb{E}[R_l] - \mathbb{E}[R_l^2]) / (L - 1)$. Substituting these results in (12), and after some simple manipulations, for $l \neq i$, (7) is found.

REFERENCES

- [1] J. Mitola III and G. Q. Maguire Jr., "Cognitive radio: making software radios more personal," *IEEE Personal Commun. Mag.*, vol. 6, no. 4, pp. 13–18, Aug. 1999.
- [2] I. F. Akyildiz, B. F. Lo, and R. Balakrishnan, "Cooperative spectrum sensing in cognitive radio networks: A survey," *Elsevier Physical Comm.*, vol. 4, pp. 40–62, Mar. 2011.
- [3] R. Gao, Z. Li, P. Qi, and H. Li, "A robust cooperative spectrum sensing method in cognitive radio networks," *IEEE Commun. Lett.*, vol. 18, no. 11, pp. 1987–1990, Nov. 2014.
- [4] D. V. Hinkley, "On the ratio of two correlated normal random variables," *Biometrika*, vol. 56, no. 3, pp. 635–639, Dec. 1969.